Quenching of Long Lifetime Emitting Fluorophores with Paramagnetic Molecules

2 AUTHORS:

Ozlem Oter
Dokuz Eylul University
24 PUBLICATIONS **386** CITATIONS

SEE PROFILE

Anne-Cécile Ribou
Université de Perpignan
35 PUBLICATIONS **527** CITATIONS

SEE PROFILE

ORIGINAL PAPER

Quenching of Long Lifetime Emitting Fluorophores with Paramagnetic Molecules

O. Oter · A-C. Ribou

Abstract In this work, we have studied quenching of the fluorescence of two well-known oxygen probes, 1-pyrene butyric acid (PBA) and tris(2,2'-bipyridine)ruthenium ([Ru$(bpy)_3]^{2+}$) by reactive oxygen species (superoxide anion, nitric oxide derivative, hydrogen peroxide) and by the O_2 molecule. Both, time-resolved and steady state fluorescence measurements were performed in solution (ethanol, dimethyl sufoxide, water) and in micelles of Sodium Dodecyl Sulfate that serve as a model for membrane-containing biological structures. We have found that only the free radicals and O_2 can actively quench for the two probes, but not the diamagnetic H_2O_2. Our data correspond to the classical Stern–Volmer equation. H_2O_2 has an effect only at high molar concentrations (>0.1 M). In contrast, effective concentrations of free radicals and O_2 that lead to quenching are in millimolar range. In conclusion, our methods allows for detecting global ROS that are small free radicals without interference from the reactive hydroxyl radical. Our data suggest that the method can be used for the quantification of ROS in individual living cells based on the measurement of fluorescence lifetime of those probes.

Keywords Fluorescence quenching · Oxygen probes · Reactive oxygen species

O. Oter
Department of Chemistry, University of Dokuz Eylul,
Tinaztepe, Buca,
Izmir, Turkey

A.-C. Ribou (✉)
Institut de Modélisation et d'Analyse en Géo-Environnements et Santé, Université de Perpignan Via Domitia,
Perpignan, France
e-mail: ribou@univ-perp.fr

Introduction

The accurate measurements of free radicals and reactive oxygen species (ROS) in vivo are essential as they contribute to the development of several human diseases. More than 60 years ago, it was suggested that fluorescence and phosphorescence quenching might be useful for measuring oxygen concentration. Nowadays, fluorescence and phosphorescence quenching is routinely employed for oxygen measurements [1]. Metal complexes such as metalloporphyrins [2], tris(bipyridyl)ruthenium(II) ([Ru(bpy)$_3$]$^{2+}$) [3], and some aromatic compounds like pyrene butyric acid (PBA) [4], have been used for this purpose in solutions [1–4], tissues [5], and in living cells [6–14]. Oxygen concentrations can be measured in living cells by measuring fluorescence intensity variations [6] or fluorescence lifetime changes [7–9]. More recently, fluorescence lifetime imaging microscopy (FLIM) with ruthenium [10–13] and porphyrin [14] complexes were developed. It was also suggested that these probes could be quenched by free radical molecules [15, 16]. Cramb et al. [15] have performed measurements with the stable TEMPO in erythrocyte ghosts and liposome suspensions. However, this approach was scarcely used, and never in living cells. In an earlier study, we developed a new method using fluorescence lifetime measurements of PBA for the detection of free radicals in single living cells [17]. Several techniques were employed to measure ROS in cultured cells and were reviewed by Halliwell and Gutteridge [18]. Fluorescent probes for free radicals and ROS detection in living cells are generated in situ by reaction of a non-fluorescent form of the probe with the ROS. Mainly, two types of fluorescent probes are employed for in vivo measurements of ROS. These are *chemiluminescent probes* such as luminol and lucigenin [19] or *fluorescent probes* such as dihydroethidium [20], BODIPY analogues [21, 22]

and the widely used dichlorofluorescin derivatives [23, 24]. Due to numerous artifacts encounter using these probes, the synthesis of new fluorescent probes is ongoing [25, 26]. So far, none of these probes are used in fluorescent lifetime experiments, thus the measurements also depend on the quantity of probe that enters the cells. Quenching measurements using fluorescence lifetime offer many advantages over intensity based measurements when working *in vivo*, they are independent of absolute intensity of the emitted light, fluorophore concentration, and artifacts arising from optical losses. We proposed to use fluorescence lifetime changes to measure ROS in cultured cells [17]. The main advantage of this method is that fluorescence lifetime measurements are independent of the absolute intensity of the emitted light, and, therefore, independent of the intracellular accumulation of the probe. Fluorescence lifetime of PBA in living cells had already permitted an evaluation of the ROS variations under various conditions [27].

While very little is known about factors which determine diffusional quenching by ROS, the mechanism by which oxygen quenches the excited state of molecules was extensively studied [28]. It was assumed that the quenching is related to the paramagnetic property of the molecule in its ground-state. In a previous paper, we assumed that among ROS, only free radicals (excluding other non paramagnetic reactive oxygen species) can act as quenchers of the oxygen probe PBA, in living cells [27]. In this study, two oxygen probes were chosen to test this assumption in solution; the aromatic PBA and the metal complex $[Ru(bpy)_3]^{2+}$. The quenching of these probes in presence of several reactive oxygen species; H_2O_2, nitric oxide radical, superoxide radical, and O_2 were investigated by time-resolved and steady state fluorescence measurements. Here, we reported, precise, artefact-free quantification of ROS by fluorescence lifetime quenching.

Experimental

Chemicals

All the compounds were from Sigma-Aldrich if not stated otherwise: the anionic surfactant sodium dodecyl sulphate (SDS), 30% solution of hydrogen peroxide, 2,2,6,6-Tetramethyl-1-biperidinyloxy free radical (TEMPO, 98%), potassium superoxide (KO_2), cis-dicyclohexano-18-crown-6 (98%), Cytochrome C from bovine heart and dimethyl sulfoxide (DMSO, 99.9% spectrophotometric grade). 1-pyrene butyric acid (PBA) was purchased from Acros Organics (Geel, Belgium). Stock solution of 5×10^{-3} M PBA was prepared in ethanol 95% or in DMSO. Tris(2,2'-bipyridine) ruthenium(II) dichloride hexahydrate ([Ru(bpy)$_3$]$^{2+}$) stock solution (3.5×10^{-6} M) was either prepared

in ethanol, DMSO or in pH 7.5 phosphate buffer. The solutions of PBA and $[Ru(bpy)_3]^{2+}$ were prepared from their stock solutions by diluting at appropriate amounts. These solutions were kept at 4°C. Xanthine oxidase was from bovine milk in lyophilized powder form (0.4–1.0 units/mg protein). The substrate xanthine was in its sodium form (≥99%), its stock solution was prepared in 1 M NaOH. The stock xanthine oxidase was prepared in cold 0.05 M pH=7.5 phosphate buffer. These stock solutions were kept at −20°C until used. All other chemicals were of analytical grade.

Fluorescence measurements

Steady-state fluorescent measurements were performed with a spectrofluorimeter (Flx, SAFAS, Monte Carlo, Monaco). Fluorescence lifetimes were determined by pulsed-lifetime measurement. The apparatus was described before [29]. In brief, the samples in a quartz cell were irradiated at 337 nm with a pulsed nitrogen laser. After collection of the emitted photons on a photomultiplier (RCA1P28), the signal was digitized with a digitizing oscilloscope (Tektronic TDS350). The analysis of the result was made considering S(t), the fluorescence response, as a function of time S(t)=G(t)*s(t). In this convolution product, G(t) represents the apparatus response for the excitation pulse and s(t) the impulse response of the fluorescence. The apparatus response can be simulated with a Gaussian curve convoluted with a time constant. The parameters of the Gaussian curve and the time constant were obtained after analysis of the response of a solution of POPOP (1,4-di-[2-(5-phenyloxazolyl)]-benzene). The experimental decay was correctly simulated with a single exponential decay using the downhill simplex method [30] to obtain time constant and the amplitude values of the two probes. After measurements of the quencher effects on time-resolved and steady state fluorescence, the data were plotted as τ_0/τ or I_0/I versus quencher concentration.

Preparation of PBA in SDS micelles

To prepare PBA in SDS micelles, 0.5 ml of 10^{-5} M PBA in ethanol were incubated at 80°C to evaporate the ethanol. A solution of 5 ml 0.01 M SDS prepared in 0.001 M pH 6.7 phosphate buffer containing 0.4 M NaCl, was added on PBA and ultrasonicated for 15 min. The prepared solution contained 10^{-6} M PBA in 10^{-2} M SDS which is ten times more concentrated than critical micelle concentration (CMC).

Oxygen quenching experiments

The pO$_2$ was controlled by mixing N$_2$ and O$_2$ gases. Gas mixtures from 0% to 100% O$_2$ were obtained by using

various oxygen and nitrogen outflows and a gas mixer (flowmeter, Aalborg, Orangeburg, NY). The gases mixture was first humidified by bubbling through pure solvent, and then directly charged into the quartz cell with a needle for 3 min. Time resolved fluorescence measurements were performed for six different oxygen levels of 100%, 75%, 50%, 21%, 13% and 0% of oxygen. The effect of the quencher on the lifetimes of the probes were evaluated in various solvents (ethanol, DMSO, pH=7.5 phosphate buffer for ruthenium complexes, and SDS micelles for PBA). The data were plotted as τ_0/τ versus oxygen pressure (atm.) and oxygen concentration (mM). To obtain the oxygen concentration in the solvents from the external oxygen pressure, the Henry constants were taken from the literature [31–33]. The oxygen solubility in SDS media was approximated by the value of aqueous solution.

Hydrogen peroxide quenching experiments

One point five milliliters of 10^{-6} M probe solutions (PBA in SDS micelles or $[Ru(bpy)_3]^{2+}$ in phosphate buffer) were placed in 1 cm quartz cells. H_2O_2 was added from freshly prepared solution in aliquots to obtain several concentrations between 5.0×10^{-4} M and 1.2 M. The quenching was analyzed with both time resolved and steady state measurements under air or nitrogen atmospheres.

TEMPO quenching experiments

One point five milliliters of 10^{-6} M probe in ethanol or in aqueous solutions (i.e. SDS micelles for PBA or phosphate buffer for $[Ru(bpy)_3]^{2+}$) were placed into 1 cm quartz cells. TEMPO stock solutions were either prepared in ethanol or in 1:1 ethanol:SDS mixture to avoid precipitation in pure SDS micelles. Stock solution of TEMPO was added in aliquots to prepare several concentrations between 5×10^{-5} M and 7×10^{-3} M. The final solutions in the buffered experiments contain less than 2% ethanol. The quenching was analyzed with both steady state and time resolved measurements under nitrogen atmosphere because TEMPO is more stable in these conditions than under atmospheric air.

Superoxide quenching experiments

Xanthine oxidase The superoxide radical (O_2^-) was generated enzymatically by a xanthine/xanthine oxidase system and the production of superoxide was monitored following the superoxide-dependent reduction of cytochrome C spectrophotometrically at 550 nm during 30 min, $\Delta\varepsilon = 28$ mM^{-1} cm^{-1} [34]. Uric acid formation was also monitored at 295 nm in order to check the enzyme activity. The reaction started by addition of xanthine oxidase into xanthine containing 0.05 M pH=7.5 potassium phosphate buffer solution. In the final mixture (2.0 ml), the concentrations were 0.1 mM ethylenediaminetetraacetic acid (EDTA), 0.01 mM cytochrome C, 0.15 mM xanthine and 0.015 U/mL xanthine oxidase. The superoxide quenching experiments with ruthenium complex and PBA were performed with the same method except that there was no EDTA or cyctochrome C in the final mixture. In the case of PBA, there was also SDS (10 mM) in the phosphate buffer. All experiments were performed in quartz cells under continuous air bubbling through the solution to keep the oxygen concentration constant.

Potassium superoxide KO$_2$ solutions were prepared just before the experiments and stabilized as in [35]. A degassed solution of dicyclohexano-18-crown-6 (0.1 M) in DMSO was added to KO$_2$ under nitrogen to obtain a final concentration of 0.05 M. 1 ml of 10^{-6} M probe in DMSO was placed in 1 cm quartz cells and degassed for several minutes. KO$_2$ was added from the freshly prepared solution in aliquots to obtain several concentrations between 5×10^{-5} M and 2×10^{-3} M. Nitrogen was bubbled into the final solution for thirty more seconds and the decay was immediately recorded. The measurements were performed within 1 min since the superoxide concentration starts to decay after this time if we continue to flow nitrogen.

Results

The deactivation of the two fluorescent probes by four different quenchers is examined in various solvents. The probes, PBA and $[Ru(bpy)_3]^{2+}$, were used between 5×10^{-7} mol/L and 5×10^{-6} mol/L in ethanol, water, DMSO, and SDS micelles. The PBA concentrations are selected to avoid the formation of excited-state complexes, excimers, thus leading to considerable simplification of the photophysics.

The simplest method for modeling the quenching phenomena is to use the Stern–Volmer equation [36]:

$$\Phi/\Phi_0 = 1 + K_{SV}[Q] \tag{1}$$

where Φ and Φ_0 are the quantum yield in the presence and absence of quencher. K_{SV} is the Stern–Volmer constant and [Q] is the quencher concentration. By using this simple equation, one assumes that there is a single type of quenching, either static or dynamic. Thus, a plot of Φ / Φ_0 versus [Q] should yield a straight line with a slope K_{SV}. Either I / I_0, the fluorescence intensities, or τ / τ_0, the fluorophore lifetimes can be plotted when steady state or lifetime based measurements are performed. In the case of static quenching involving the ground state, the fluores-

cence intensity alone should decrease in the presence of quenchers while after a dynamic quenching of the excited state both lifetimes and intensities will decrease. In this case, K_{SV} is the product of τ_0 and kq, the bimolecular quenching rate constant for the reaction of the excited state with the quencher Q. This quenching rate constant is usually related to the diffusion controlled limit through the quenching efficiency, γ, and the diffusion constant, k_{diff}.

Oxygen quenching

Oxygen is known to be an effective collisional quencher, and this ability to quench fluorescent molecule is presumed to be due to its paramagnetic property. The excited molecule is deactivated non radiatively to its ground state due to the collisions with the oxygen. However, excited molecules, especially on their triplet state, are well known to generate singlet oxygen via energy transfer to the ground state of the oxygen molecule from the excited state of the probe. The employed probes, after excitation, are in excited states of different multiplicities. The deactivation mechanisms of the two probes by O_2 should be different, with a more complex S_1-state quenching of the pyrene derivative than the T_1-state quenching of the ruthenium complex. Thus, different competing deactivation processes can happen, leading directly to the ground-state S_0 with or without $O_2(^1\Delta g)$ formation [37]. Eventually, O_2 quenches excited states of both multiplicities, with variable rate constants close to the diffusion-controlled limit. In this study, in order to compare the quenching with reactive oxygen species, the quenching of the two probes by oxygen was investigated in several solvents (ethanol, water, DMSO) and SDS micelles. The increase of O_2 concentration both in PBA and $[Ru(bpy)_3]^{2+}$ solutions results in a decrease of the lifetime of the probes. To calculate the solubility of oxygen in the various solvents, Henry constants are obtained from Chebbo et al. [31], Tokugawa [32] and Franco et al. [33]. We use values of 116, 781, and 636 (atm.L.mol^{-1}) in ethanol 95%, water, and DMSO,

respectively. The lifetime plotted according to Stern-Volmer presents a linear behaviour in all case. The corresponding slopes, K_{SV} are presented in Table 1. From K_{SV}, we calculate the quenching rate constant, kq, close to diffusion-controlled limit for PBA. kq is ranging from 0.8 L. mol^{-1}.s^{-1} to 1.6×10^{10} L.mol^{-1}.s^{-1} depending on the solvent. PBA quenching by O_2 in SDS micelles, kq= 1.0×10^{10} L.mol^{-1}.s^{-1}, is similar to the quenching constant we already reported in liposome suspensions [17]. Indeed, SDS micelles, like liposome suspensions, are supposed to provide a hydrophobic environment to PBA. Liposome suspensions were previously used as a simplified model for biological membranes since PBA was shown to integrate into the cytosolic membrane [17]. Here, we use SDS micelles as a model for PBA measurements to mimic biological media whenever the stability of the quencher allows it. In contrast, the localization of $[Ru(bpy)_3]^{2+}$ in cells should correspond to a hydrophilic environment possibly at the surface of plasma membrane or in endocytic vesicles [8]. Thus, the experiments are preferentially performed in water. Because of the poor stability of some of the free radical molecules in water, some of the measurements were also performed in ethanol or in DMSO. The quenching constant for $[Ru(bpy)_3]^{2+}$ in water, 2.5×10^9 L.mol^{-1}s^{-1}, is consistent with literature values [38]. One can assume, considering the longer lifetime of ruthenium complexes compared with aromatic compounds under nitrogen atmosphere that the O_2 detection range with such a probe will be higher. However, when compared with PBA, the quenching constant of $[Ru(bpy)_3]^{2+}$ is ten times lower in ethanol and three times lower in DMSO. Therefore, the O_2 concentration detected are rather similar.

Superoxide anion

The generation of free radical O_2^- is first obtained with an enzymatic procedure by mixing xanthine and xanthine oxidase and the generated amount is measured by a cytochrome c reduction method [39]. This catalyzed

Table 1 Fluorescence decay constants and oxygen quenching constants of PBA (10^{-6} M) and $[Ru(bpy)_3]^{2+}$ (5×10^{-6} M) in different media

PBA	τ_o (ns)	τ_{air} (ns)	K_{SV} (atm^{-1})	kq (L mol^{-1} s^{-1})
H$_2$O	138	106	1.5[a]	0.8×10^{10}
SDS micelle	232	146	3.00 (0.01)[b]	1.0×10^{10}
DMSO	136 (*freshly prepared: 154*)	85.9	3.4 (0.3)	1.6×10^{10}
Ethanol	220	31	25[a]	1.3×10^{10}
[Ru(bpy)$_3$]$^{2+}$	τ_o (ns)	τ_{air} (ns)	K_{SV} (atm^{-1})	kq (L mol^{-1-1})
H$_2$O	580	395	1.81 (0.04)	2.5×10^9
DMSO	1,094	445	8.7 (0.1)	5.0×10^9
Ethanol	694	296	7.1 (0.1)	1.2×10^9

[a] from Ribou et al., 2004 [17].
[b] X(ΔX):ΔX=(K_{SVmax}−K_{SVmin})/2.

reaction takes several minutes to generate appreciable quantities of O_2^-. According to the literature the reaction must proceed for at least 30 min to accumulate a high quantity of superoxide anion. However, we calculated that the initial production rate of superoxide anion by this method corresponds to a maximum level of 120 nM/s. This is not sufficient to generate a local concentration that is detectable by our system.

Millimolar concentrations of superoxide anion were then prepared from KO_2 via a chemical procedure. O_2^- is not stable in aqueous solution but is stable for several minutes in nitrogen-degased DMSO with added crown-ether [40]. The lifetime measurements performed in water with [Ru(bpy)$_3$]$^{2+}$ shows that half of the radical is already destroyed after about 30 s. Thus, the quenching efficiency of superoxide anion was studied in DMSO. The fluorescence decay of the two probes was recorded after addition of the free radical at increasing concentrations. The variation of the lifetime ratio (τ_0/τ) versus KO_2 concentrations are plotted for PBA and [Ru(bpy)$_3$]$^{2+}$ (Fig. 1). Data obtained in the same solvent with oxygen as quencher are added for comparison. The values of kq are obtained from the linear analyses of the plots and are summarized in Table 2. It is worth noting, that PBA in DMSO transforms slowly when left in the dark, or rapidly after addition of an equimolar amount of KO_2. We observe that these two phenomena give new compounds with identical spectral properties. These now possess new spectrum and a new lifetime, 136 ns, that is taken as τ_0 value in the analysis. The fluorescence spectra show a change of the relative intensities of the vibronic bands I (376 nm) and II (395 nm) (data not shown). Such spectral changes are often related to the solvent environment and can be monitored by the measurements of the ratio II/I. We calculate a ratio of 0.85 for freshly prepared solution and 0.81 later or after KO_2 addition. The decrease of this ratio had first suggested an increase in polarity of the environment of the pyrene moiety. To better understand this phenomenon, we decided to reproduce the experiments with pyrene alone. Pyrene intensity and lifetime is stable in DMSO and after addition

of KO_2. The lifetime without quenchers is 277.5 ns. Consequently, we attribute the behaviour of PBA in this experiment to an effect of the pyrene side-chain. With pyrene as a probe, we obtain a ratio k_{O2}/k_Q of 3. This ratio is more than twofold higher for PBA ($k_{O2}/k_Q=8$, Table 2). This suggests that the quenching of the pyrene moiety by the superoxide anion takes place more rapidly without the side-chain. For [Ru(bpy)$_3$]$^{2+}$, the ratio k_{O2}/k_Q was lower than one implying that the quenching with superoxide anion is higher than that with molecular oxygen. This can possibly be explained by a charge effect because, since the probe is positively charged, probe and quencher will be oppositely charged. Thus, electrostatic attraction occurs between [Ru(bpy)$_3$]$^{2+}$ and O_2^- and improves quenching.

Hydroxyl radical

The superoxide anion is not stable enough in aqueous solution to allow direct quantification. Therefore, we can assume that the highly reactive radical OH° will not survive long enough to be detected in solutions by our method. This radical, that may be formed in vivo, reacts with whatever is in its immediate vicinity within microseconds [18]. A mixture of H_2O_2 with iron complexes (Fenton reaction) is commonly used in order to degrade polycyclic aromatic hydrocarbons such as pyrene [41, 42]. Reactions and degradations of ruthenium complexes with OH° are also well documented [43]. In cells, all other biomolecules will react quickly with OH° and will compete with the fluorescent probes. It is unlikely that a high concentration of the probes will be found at the site of OH° generation. Indeed, we never detected a significant decrease of PBA intensity that would indicate probe degradation during the experiment performed in living cells [17].

Hydrogen peroxide

The measurements are performed in nitrogen-degased SDS micelles for PBA, and in water for [Ru(bpy)$_3$]$^{2+}$. For lifetime-based measurements, quenching by the non-radical

Fig. 1 Variations of the lifetime ratio (τ_0/τ) versus quencher concentrations in DMSO at 25°C. On the left, Pyrene butyric acid (PBA) at 5×10^{-7} M; on the right, Tris(2,2'-bipyridine)ruthenium(II) ([Ru(bpy)$_3$]$^{2+}$) at 1×10^{-6} M. Full symbols: KO_2 and Hollow symbols: O_2. The data are the mean values of three measurements
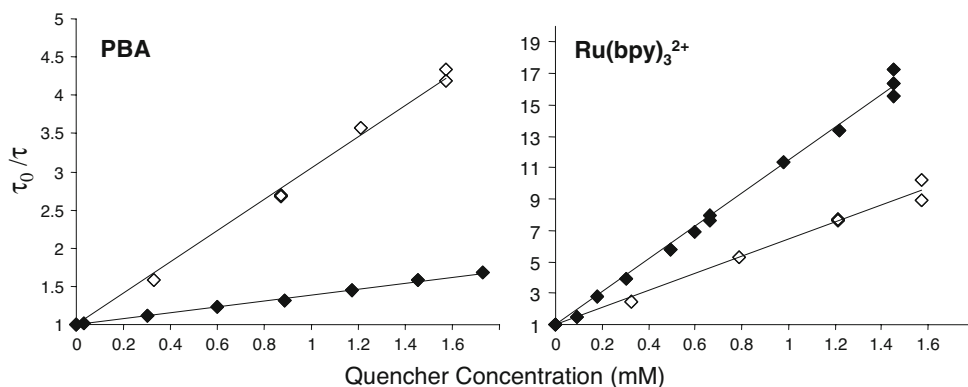
Table 2 Fluorescence decay constants and quenching constants of PBA (10^{-6} M) and $[Ru(bpy)_3]^{2+}$ (5×10^{-6} M) for different quenchers under nitrogen atmosphere

PBA	τ_o (ns) (solvent)	τ_Q (ns) [Q]=1 mM	K_{SV} (mM^{-1})	kq (L mol^{-1} s^{-1})	k_{O2}/k_Q[a]
O_2^- : KO_2	136 (DMSO)	106	0.24 (0.04)[b]	1.8×10^9	8
H_2O_2	232 (SDS micelle)	no change	0.0012 (0.0004)	4.7×10^3	10^6
TEMPO (~NO·)	220 (ethanol)	140	0.6 (0.2)	2.9×10^9	5
	232 (SDS micelles)	–	1.1 (0.1)	4.9×10^9	2
$[Ru(bpy)_3]^{2+}$	τ_o (ns) (solvent)	τ_Q (ns) [Q]=1 mM	K_{SV} (mM^{-1})	kq (L mol^{-1} s^{-1})	k_{O2}/k_Q
O_2^- : KO_2	1,094 (DMSO)	97	10.0 (0.3)	9×10^9	0.5
H_2O_2	580 (H_2O)	no change	0.0002 (0.0001)	0.3×10^3	10^5
TEMPO (~NO·)	834 (ethanol)	745	0.15 (0.02)	1.7×10^8	7
	606 (H_2O)	577	0.04 (0.01)	0.7×10^8	35

[a] k_{O2} and k_Q are the quenching rate constants for oxygen molecule, O_2, and reactive oxygen species, Q.
[b] $X(\Delta X)$: $\Delta X=(K_{SVmax}-K_{SVmin})/2$.

H_2O_2 does not occur under 0.1 molar concentrations for both probes (Fig. 2, left). The order of magnitude of kq is 5.0×10^3 $L.mol^{-1}s^{-1}$ for PBA and 3.0×10^2 for $[Ru(bpy)_3]^{2+}$ with a correlation R^2 value in the range 0.94–0.98 (Table 2). Such a constant is more than ten times lower than the constant already reported for steady state experiments with ruthenium complex. Indeed, when performing steady state measurements with $[Ru(bpy)_3]^{2+}$ according to the protocol of Choi and Bard [44], we simulate our data with a linear slope K_{SV} equal to 3.3 M^{-1} (2.3 M^{-1} in [44]). However, when increasing the quencher concentrations (0.1–0.4 M), the Stern–Volmer plot exhibits a downward curvature and the slope is reduced to 0.4 M^{-1}. PBA was not previously studied, although Cramb and Beck [15] reported quenching of Benzo(a)pyrene in SDS micelles by high H_2O_2 concentration. Again, we obtain K_{SV} in steady state measurements (0.09 mM^{-1}) hundred times higher than in lifetime based measurements (0.0012 mM^{-1}). While PBA photo-degradation is less than 5% after 2 h irradiation at 337 nm, we observe an increase of the photo-degradation after addition of H_2O_2 (Fig. 2, inset). Altogether, the fluorescent spectrum is changed (Fig. 2, right) and the ratio II/I varies from 0.93 to 1.14 after H_2O_2 addition. We assume this degradation to be due to OH° formation during irradiation at 337 nm. Degradation of the fluorescent molecule on its ground-state will not affect the lifetime of the probe and explains our results (Table 2). Kubat et al [45] already followed the degradation of pyrene after irradiation at 334 nm through the possible formation of OH°. In the case of ruthenium complex, we observed minor degradation of similar magnitude (less than 13%) under irradiation, with and without H_2O_2.

Nitrogen oxide

We study the stable, nitroxyl radical 2,2,6,6-tetramethylpiperidine-N-oxyl (TEMPO). Since the early 80's, TEMPO was frequently studied as paramagnetic fluorescence
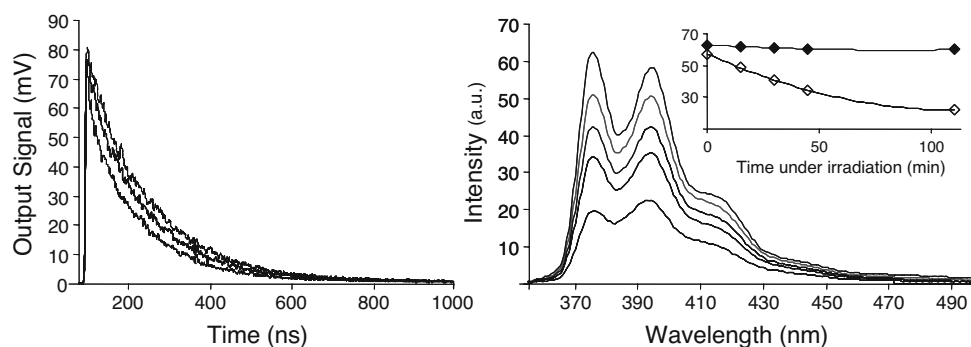

Fig. 2 Fluorescence decay profiles (*left*) and intensity spectra (*right*) of PBA in SDS micelles for several H_2O_2 concentrations. Left: two additions 0.12 M and 0.29 M; right: one single addition 6 mM followed by irradiation (see inset). The decays are recorded under air atmosphere. Inset: fluorescent intensity decrease under irradiation versus time, after addition of H_2O_2 (hollow symbols) and without addition (full symbols)

quencher, with $[Ru(bpy)_3]^{2+}$ as well as pyrene [46]. Pyrene and PBA were later studied in solution [47], micelles [48], and membranes [49]. The quenching takes place with TEMPO concentrations lower than millimolar. We present the data obtained in ethanol for both probes with TEMPO and O_2 as quenchers (Fig. 3). The experiments are also performed in SDS micelles for PBA and water solution for $[Ru(bpy)_3]^{2+}$. In all cases, the lifetime plotted according to Stern–Volmer present a linear behaviour. The slope allows to calculate a quenching constant of 2.9×10^9 L.mol^{-1}.s^{-1} for PBA, and 1.7×10^8 L.mol^{-1}.s^{-1} for the ruthenium complex in ethanol. The latter is very close to the one calculated by Lymar et al [46] for slightly bulky free radical in ethanol. The ratio k_{O2}/k_Q is quite similar for both probes in ethanol and is calculated to be five and seven for PBA and for $[Ru(bpy)_3]^{2+}$, respectively (Table 2). In SDS micelles and water, TEMPO is introduced in small amounts in ethanol but the final ethanol concentrations never exceeds 2%. The value of 4.9×10^9 L.mol^{-1}.s^{-1} is two times lower than the one already published [48]. However, Angelescu and Vasilescu used a slightly different protocol. They calculated the kq value from a single addition of TEMPO at 0.9 mM. The result presents a high uncertainty that can explain the difference with our observations. For PBA, the ratio k_{O2}/k_Q is 5 in ethanol and less than 2 in SDS micelles. For $[Ru(bpy)_3]^{2+}$ in water, the quenching is low (kq=0.7×10^8 L.mol^{-1}.s^{-1}) and we obtain an unexpected ratio k_{O2}/k_Q of 35. In this case, we can doubt about the stability of TEMPO in pure water as solvent.

Steady state measurements are also performed in ethanol, SDS and water. Unlike H_2O_2, degradation of the probe PBA after addition of TEMPO and after irradiation is not detected. We compared the data obtained with steady state and lifetime based experiments for PBA and [Ru(bpy)$_3$]$^{2+}$. The ratio between Stern–Volmer constants obtained in the two experiments is found in all cases in the range of 1.1–1.2.

Nitric oxide is the principal and smallest nitrogen-oxygen reactive species produced in cells. The small NO° has a higher diffusion coefficient than the large TEMPO. Quenching of the fluorescence of pyrene derivatives by nitric oxide and oxygen were already evaluated [16]. In solution, both showed the same quenching efficiency with a ratio k_{O2}/k_Q closed to one. Thus, we suppose that the two fluorescent probes, PBA and $[Ru(bpy)_3]^{2+}$, will show higher sensitivity for nitric oxide in cells when compared to TEMPO.

Discussion

Because of the importance of reactive oxygen species for many biological processes, detecting and quantifying them is an essential step for the understanding of their impact on the function of cells and tissues. Our laboratory already demonstrated that ROS can act as quenchers for oxygen probes in living cells. But several questions were raised. First of all, here we prove that free radicals can act as quenchers. The mechanism of quenching of the free radical is certainly related to its paramagnetic properties similar to those of the oxygen molecule. We observed that comparable quencher concentrations can be used for free radical and oxygen molecules. The key point is that in living cells and in solutions, the fluorescent probes will not detect millimolar quantities of H_2O_2 or other diamagnetic reactive oxygen species but only free radicals. Indeed, we show that we must add H_2O_2 concentrations higher than 0.1 M to detect the quenching. Among free radicals, OH° is highly reactive and will react rapidly after its formation and before diffusing. Because of the need of diffusion in collisional quenching, we assume that our measurements are not influenced by OH°. It is reasonable to assume that in cells where the quenchers have to be small enough to diffuse and to reach the probe, we will not detect lipid peroxidation. The diffusion of the large free radical that is stacked in membrane will not occur. The quenching will happen only if the probe is already in the vicinity of the lipid-derived radical. At low concentrations of the probe (10^{-6} M) this

Fig. 3 Variations of the lifetime ratio (τ_0/τ) versus quencher concentrations in ethanol at 25°C. On the *left*, Pyrene butyric acid (PBA) at 1×10^{-6} M; on the *right*, Tris(2,2'-bipyridine)ruthenium(II) ([Ru(bpy)$_3$]$^{2+}$) at 1×10^{-6} M. Full symbols: TEMPO and Hollow symbols: O_2. The measurements are performed in triplicate. Data with PBA and oxygen are from [17] and are performed at 21°C
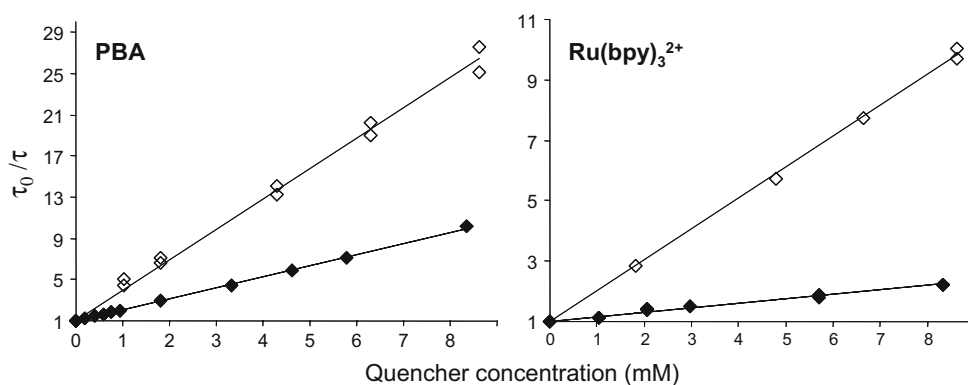
situation is unlikely. To summarize, with oxygen probes in cells, we will be able to detect global ROS variations that are due to changes in the amounts of small free radicals but not OH°.

In general, dynamic quenching is treated by the classical model for diffusion-controlled reaction (Smoluchowski model). It depends on the rate of diffusion between the reactants (related to the viscosity of the solvent) and on their size. In this model, the reactants are supposed to be homogeneously distributed and to experience no electrostatic interaction. In addition, the efficiency of the reaction (i.e. collision) is assumed to be unit. Some of these assumptions are not fulfilled in our experiments. We can doubt about the homogeneous distribution in the case of SDS micelles and membranes and we can expect electrostatic interaction between the positively charged probe [Ru (bpy)$_3$]$^{2+}$ and charged radicals such as superoxide anion. We have observed different results for the quenching rate constants of the two probes. With oxygen molecules, we always found that kq values are higher for PBA compared to [Ru(bpy)$_3$]$^{2+}$ (three to ten times). We doubt that the size difference alone of the two probes and consequently the diffusion of the two probes, can explain these results. These results might possibly be explained by a lower quenching efficiency of the ruthenium complex. As a consequence, O$_2$ detection range will not be improved with the long lifetime ruthenium complex. However, for [Ru(bpy)$_3$]$^{2+}$, we observed the highest quenching constant (kq=9×10^9 L.mol^{-1}. s^{-1}) with superoxide anion. Thus, we conclude that ruthenium complex will be a more suitable probe for detection of this free radical and consequently global ROS. Further measurements in living cells must be done to confirm this assumption.

Here, we showed that among the reactive oxygen species, free radicals can quench the fluorescence of oxygen probes in millimolar concentrations. Altogether, we showed that ROS variation will influence the quantification of oxygen with fluorescent probes in living material. We recently used this new method to quantify global ROS variation in single living cells with the probe PBA [50]. We assume that this method can be extended to all oxygen fluorescent probes such as ruthenium or metalloporphyrin complexes that were frequently used in cells for oxygen quantification. However, one has to keep in mind that oxygen variation will produce artefacts in the free radical quantification and vice versa. In addition, we can expect that additional information, on H$_2$O$_2$ and lipid peroxidation [21–24], can be obtained when using our approach together with other methods.

References

1. Borisov SM, Wolfbeis OS (2008) Optical sensors. Chem Rev 108 (2):423–461 doi:10.1021/cr068105t
2. Lo L-W, Koch CJ, Wilson DF (1996) Calibration of oxygen-dependent quenching of the phosphorescence of Pd-meso-tetra(4-Carboxyphenyl)porphirine: a phosphor with general application for measuring oxygen concentration in biological systems. Anal Biochem 236(1):153–160 doi:10.1006/abio.1996.0144
3. Sasso MG, Quina FH, Bechara EJH (1986) Ruthenium(II) Tris (bipyridyl) ion as a luminescent probe for oxygen uptake. Anal. Biochem. 156(1):239–243 doi:10.1016/0003-2697(86)90178-8
4. Vaughan WM, Weber G (1970) Oxygen quenching of pyrenebutyric acid fluorescence in water. A dynamic probe of the microenvironment. Biochem 9(3):464–473 doi:10.1021/bi00805a003
5. Vanderkooi JM, Erecinska M, Silver IA (1991) Oxygen in mammalian tissues: methods of measurement and affinities of various reactions. Am J Physiol-Cell Physiology 260(6 29/6):C1131–C1150
6. Benson DM, Knopp JA, Longmuir IS (1980) Intracellular oxygen measurements of mouse liver cells using quantitative fluorescence video microscopy. Biochim Biophys Acta 591(1):187–197 doi:10.1016/0005-2728(80)90232-7
7. Huglin D, Seiffert W, Zimmermann HW (1995) Time-resolved microfluorometric study of the binding sites of lipophilic cationic pyrene probes in mitochondria of living HeLa cells. J Photochem Photobiol B 31(3):145–158 doi:10.1016/1011-1344(95)07191-1
8. Dobrucki JW (2001) Interaction of oxygen-sensitive luminescent probes Ru(phen)32+ and Ru(bipy)32+ with animal and plant cells in vitro. Mechanism of phototoxicity and conditions for non-invasive oxygen measurements. J Photochem Photobiol B 65(2–3):136–144 doi:10.1016/S1011-1344(01)00257-3
9. Mik EG, Stap J, Sinaasseppel M, Beek JF, Aten JA, van Leeuwen TG, Ince C (2006) Mitochondrial PO$_2$ measured by delayed fluorescence of endogenous protoporphyrinIX. Nat Methods 3 (11):939–945 doi:10.1038/nmeth940
10. Suhling K, French PM, Phillips D (2005) Time-Resolved fluorescence microscopy. Photochem. Photobiol Sci 4(1):13–22 doi:10.1039/b412924p
11. Gerritsen HC, Sanders R, Draaijer A, Ince C, Levine YK (1997) Fluorescence Lifetime Imaging of Oxygen in Living cells. J Fluo 7(1):11–15 doi:10.1007/BF02764572
12. Zhong W, Urayama P, Mycek M-A (2003) Imaging fluorescence lifetime modulation of a ruthenium-based dye in living cells: the potential for oxygen sensing. J Appl Phys 36(14):1689–1695
13. Sud D, Zhong W, Beer DG, Mycek M-A (2006) Time-resolved optical imaging provides a molecular snapshot of altered metabolic function in living human cancer cell models. Opt Express 14(10):4412–4426 doi:10.1364/OE.14.004412
14. O'Riordan TC, Fitzgerald K, Ponomarev GV, Mackrill J, Hynes J, Taylor C et al (2007) Sensing intracellular oxygen using near-infrared phosphorescent probes and live-cell fluorescence imaging. Am J Physiol Regul Integr Comp Physiol 292:1613–1620 doi:10.1152/ajpregu.00707.2006
15. Cramb DT, Beck SC (2000) Fluorescence quenching mechanisms in micelles: the effect of high quencher concentration. J Photochem Photobiol A 134(12):87–95 doi:10.1016/S1010-6030(00)00249-5
16. Denicola A, Souza JM, Radi R, Lissi E (1996) Nitric oxide diffusion in membranes determined by fluorescence quenching. Arch Biochem Biophys 328(1):208–212 doi:10.1006/abbi.1996.0162
17. Ribou A-C, Vigo J, Salmon J-M (2004) Lifetime of fluorescent pyrene butyric acid probe in single living cells for measurement of

oxygen fluctuation. Photochem Photobiol 80(2):274–280 doi:10.1562/2004-03-11-RA-109.1

18. Halliwell B, Gutteridge J (2007) Free Radical in biology and medicine, 4th edn. Oxford, pp 302–308

19. Li Y, Zhu H, Trush MA (1999) Detection of mitochondria-derived reactive oxygen species production by the chemilumigenic probes lucigenin and luminal. Biochem Biophys Acta-Gen Subjects 1428 (1):1–12

20. Budd SL, Castilho RF, Nicholls DG (1997) Mitochondrial membrane potential and hydroethidine-monitored superoxide generation in cultured cerebellar granule cells. FEBS Lett 415 (1):21–24 doi:10.1016/S0014-5793(97)01088-0

21. Drummen GPC, Gadella BM, Post JA, Brouwers JF (2004) Mass Spectroscopic characterization of the oxidation of the fluorescent lipid peroxidation reporter molecule C1-BODIPY581/591. Free Radic Biol Med 36(12):1635–1644 doi:10.1016/j.freerad biomed.2004.03.014

22. MacDonald ML, Murray IVJ, Axelsen PH (2007) Mass spectrometric analysis demonstrates that BODIPY 581/591 C11 overestimates and inhibits oxidative lipid damage. Free Radic Biol Med 42(9):1392–1397 doi:10.1016/j.freeradbiomed.2007.01.038

23. Ohashi T, Mizutani A, Murakami A, Kojo S, Ishii T, Taketani S (2002) Rapid oxidation of dichlorodihydrofluorescin with heme and hemoproteins: formation of the fluorescein is independent of the generation of reactive oxygen species. FEBS Lett 511(1–3):21–27 doi:10.1016/S0014-5793(01)03262-8

24. Rota C, Fann YC, Mason RP (1999) Phenoxyl free radical formation during the oxidation of the fluorescent dye 2′,7′-dichlorofluorescein by horseradish peroxidase. Possible consequences for oxidative stress measurements. J Biol Chem 274 (40):28161–28168 doi:10.1074/jbc.274.40.28161

25. Setsukinai K, Urano Y, Kikuchi K, Higuchi T, Nagano T (2000) Fluorescence switching by o-dearylation of 7-arylocoumarins. Development of novel fluorescence probes to detect reactive oxygen species with high selectivity. J Chem Soc, Perkin Trans 2 (12):2453–2457 doi:10.1039/b006449l

26. Chang MCY, Pralle A, Isacoff EY, Chang CJ (2004) A Selective, Cell-Permeable Optical Probe for Hydrogen Peroxide in Living Cells. J Am Chem Soc 126(47):15392–15393 doi:10.1021/ja0441716

27. Rharass T, Vigo J, Salmon J-M, Ribou A-C (2006) Variation of 1-pyrenebutyric acid fluorescence lifetime in single living cells treated with molecules increasing or decreasing reactive oxygen species levels. Anal Biochem 357(1):1–8 doi:10.1016/j.ab.2006.07.009

28. Wilkinson F, McGarvey DJ, Olea AF (1993) Factors Governing the Efficiency of Singlet Oxygen Production during Oxygen Quenching of Singlet and Triplet States of Anthracene Derivatives in Cyclohexane Solution. J Am Chem Soc 115(25):12144–12151 doi:10.1021/ja00078a062

29. Ribou A-C, Vigo J, Kohen E, Salmon J-M (2003) Microfluorimetric study of oxygen dependence of (1″-pyrene butyl)-2-rhodamine ester probe in mitochondria of living cells. J. Photochem. Photobiol. B Biol 70(2):107–115 doi:10.1016/S1011-1344 (03)00072-1

30. Nelder JA, Mead R (1965) A simplex method for function minimization. Comput J 7:303–333

31. Chebbo M, Catte M, Richard C (1993) Measurement and prediction of oxygen solubility water-alcohol media. Recent Prog Genie Procedes 7(27):379–384

32. Tokugawa J (1975) Solubilities of oxygen, nitrogen, and carbon dioxide in aqueous alcohol solutions. J Chem Eng Data 20(1):41–46 doi:10.1021/je60064a025

33. Franco C, Olmsted J (1990) Photochemical determination of the solubility of oxygen in various media. Talanta 37(9):905–909 doi:10.1016/0039-9140(90)80251-A

34. Margoliash E, Frohwirt N, Weiner E (1959) A study of the cytochrome c haemochromogen. Biochem J 71(3):559–572

35. Valentine JS, Curtis AB (1975) A convenient preparation of solutions of superoxide anion and the reaction of superoxide anion with a copper(II) complex. J Am Chem Soc 97(1):224–226 doi:10.1021/ja00834a058

36. Stern O, Volmer M (1919) The extinction period of fluorescence. Phys Z 20:183–188

37. Schweitzer C, Schmidt R (2003) Physical mechanisms of generation and deactivation of singlet oxygen. Chem Rev 103 (5):1685–1757 doi:10.1021/cr010371d

38. Demas JN, Diemente D, Harris EW (1973) Oxygen quenching of charge-transfer excited states of ruthenium(II) complexes. Evidence for singlet oxygen production. J Am Chem Soc 95 (20):6864–6865 doi:10.1021/ja00801a073

39. McCord JM, Fridovich I (1969) Superoxide dismutase. An enzymatic function for erythrocuprein (homocuprein). J Biol Chem 244(22):6049–6055 adapted by Sigma-Aldrich

40. Lokesh BR, Cunningham ML (1986) Further studies on the formation of oxygen radicals by potassium superoxide in aqueous medium for biochemical investigations. Toxicol Lett 34(1):75–84 doi:10.1016/0378-4274(86)90147-5

41. Wen S, Zhao J, Sheng G, Fu J, Peng P (2003) Photocatalytic reactions of pyrene at TiO2/water interfaces. Chemosphere 50 (1):111–119 doi:10.1016/S0045-6535(02)00420-4

42. Flotron V, Delteil C, Padellec Y, Camel V (2005) Removal of sorbed polycyclic aromatic hydrocarbons from soil, sludge and sediment samples using the Fenton's reagent process. Chemosphere 59 (10):1427–1437 doi:10.1016/j.chemosphere.2004.12.065

43. Maliyackel AC, Waltz WL, Lilie J, Woods RJ (1990) Radiolytic study of the reactions of hydroxyl radical with cobalt(III), iron(II), and ruthenium(II) complexes containing 2,2'-bipyridyl and cyano ligands. Inorg Chem 29(2):340–348 doi:10.1021/ic00327a037

44. Choi J-P, Bard AJ (2005) Electrogenerated chemiluminescence (ECL) 79. Reductive-oxidation ECL of tris(2,2'-bipyridine)ruthenium(II) using hydrogen peroxide as a coreactant in pH 7.5 phosphate buffer solution. Anal Chim Acta 541(1–2):143–150

45. Kubát P, Civiš S, Muck A, Barek J, Zima J (2000) Degradation of pyrene by UV radiation. J Photochem Photobiol A: Chem 132 (12):33–36

46. Lymar SV, Kokorin AI, Parmon VN (1981) Deactivation of electronic excited states of stable nitroxyl biradicals. Izv. Akad. Nauk SSSR [Khim] 11:2616–2618

47. Suzuki T, Obi K (1995) Evidence for enhanced intersystem crossing on pyrene fluorescence quenching with stable free radicals. Chem Phys Lett 246(1):130–134 doi:10.1016/0009-2614(95)01138-Y

48. Angelescu D, Vasilescu M (2001) Quenching of pyrene derivatives' fluorescence by nitroxide radicals in sodium dodecyl sulfate micellar solutions. J Colloid Interface Sci 244(1):139–144 doi:10.1006/jcis.2001.7900

49. Johnson DA, Nguyen B, Bohorquez AF, Valenzuela CF (1999) Paramagnetic fluorescence quenching in a model membrane: a consideration of lifetime and temperature. Biophys Chem 79(1):1–9 doi:10.1016/S0301-4622(99)00036-8

50. Rharass T, Vigo J, Salmon J-M, Ribou A-C (2008) Reactive oxygen species in anti-tumoral activity of adriamycin: hypoxic and oxygenated cells. Free Radic Res 42(2):124–134 doi:10.1080/10715760701834552